Coupling of vinculin to F-actin demands Syndecan-4 proteoglycan

R.P. Cavalheiro [a], M.A. Lima [a,b], T.R. Jarrouge-Bouças [a], G.M. Viana [a], C.C. Lopes [a,c], V.J. Coulson-Thomas [a,d], J.L. Dreyfuss [a,e], E.A. Yates [a,b], I.L.S. Tersariol [a] and H.B. Nader [a]

a - Disciplina de Biologia Molecular, *Departamento de Bioquímica, Escola Paulista de Medicina, Universidade Federal de São Paulo, SP, Brazil*
b - Institute of Integrative Biology, *Department of Biochemistry, University of Liverpool, Liverpool, UK*
c - Instituto de Ciências Ambientais, *Químicas e Farmacêuticas, Universidade Federal de São Paulo, Diadema, SP, Brazil*
d - University of Houston, *College of Optometry, The Ocular Surface Institute (TOSI), Houston, USA*
e - Grupo Interdisciplinar de Ciências Exatas em Saúde, *Universidade Federal de São Paulo, SP, Brazil*

Correspondence to H.B. Nader: *at: Rua Três de Maio, 100, Vila Clementino, SP 04044-020, Brazil.*
hbnader.bioq@epm.br.
http://dx.doi.org/10.1016/j.matbio.2016.12.006

Abstract

Syndecans are heparan sulfate proteoglycans characterized as transmembrane receptors that act cooperatively with the cell surface and extracellular matrix proteins. Syn4 knockdown was performed in order to address its role in endothelial cells (EC) behavior. Normal EC and shRNA-Syn4-EC cells were studied comparatively using complementary confocal, super-resolution and non-linear microscopic techniques. Confocal and super-resolution microscopy revealed that Syn4 knockdown alters the level and arrangement of essential proteins for focal adhesion, evidenced by the decoupling of vinculin from F-actin filaments. Furthermore, Syn4 knockdown alters the actin network leading to filopodial protrusions connected by VE-cadherin–rich junction. shRNA-Syn4-EC showed reduced adhesion and increased migration. Also, Syn4 silencing alters cell cycle as well as cell proliferation. Moreover, the ability of EC to form tube-like structures in matrigel is reduced when Syn4 is silenced. Together, the results suggest a mechanism in which Syndecan-4 acts as a central mediator that bridges fibronectin, integrin and intracellular components (actin and vinculin) and once silenced, the cytoskeleton protein network is disrupted. Ultimately, the results highlight Syn4 relevance for balanced cell behavior.

Introduction

Understanding how single molecular entities function and what their specific role is in a given biological process remains a central question in biology. Syndecans are heparan sulfate proteoglycans (HSPGs) that form an evolutionarily conserved family of type I transmembrane proteins present, ubiquitously, at the cell surface that act as cell-cell and cell-extracellular matrix (ECM) communicators. They are required for normal cell function once they may receive and transduce signals to both extra- and intracellular compartments [11,14,28,50].

The dynamic assembly and disassembly of the cytoskeletal protein network coordinates several cell behaviors ranging from cell shape to adhesion, migration and division and its disruption is a key factor in numerous cell function abnormalities. Syndecan-4 (Syn4) is required for proper focal adhesion (FA) formation and regulation [40,47]. Nonetheless, little is known about whether Syn4 loss affects specific proteins from the FA complex or the complex as a whole.

FAs are specialized zones of tight cell-matrix interaction located at the termini of cytoskeleton actin stress fibers, and are important signaling centers

Please cite this article as: R.P. Cavalheiro, et al., Coupling of vinculin to F-actin demands Syndecan-4 proteoglycan, Matrix Biol (2016), http://dx.doi.org/10.1016/j.matbio.2016.12.006

[4,28,33,51], where integrins and cell surface HSPGs are crucial for proper actin stress fiber organization [7,12,15,16,19,25,48]. Hence, Syn4 binding to ECM components such as fibronectin (FN), laminin, vitronectin and collagen, as well as actin-associated molecules at both the intracellular and the cell surface compartments, determine cell phenotype through the modulation of distinct signal-transduction events.

Herein, to better understand the role of Syn4 in cellular behavior via the disruption of FA and cytoskeleton arrangement, Syn4 knockdown was performed in endothelial cells (ECs). Morphological and functional cellular characteristics including were then compared.

Employing state-of-the-art microscopy, and single molecule localization super-resolution microscopy, the cellular alterations that led to the aberrations of Syn4 deficient cells were also dissected. Selective alterations in the cytoskeleton protein network assembly were shown in which the decoupling of vinculin from F-actin filaments, as the result of Syn4 loss, was revealed by nanoscopy. Further changes were also found related to cell surface and ECM protein expression and deposition. Together, the data show how normal cell behavior relies on proper cytoskeleton assembly and implicates Syn4 as a crucial signaling center for proper communication between intracellular, cell surface and ECM components.

Results

Loss of Syndecan-4 alters downstream signaling and actin network

Wild type ECs were transfected as described in Methods and the Syn4 knockdown was confirmed by real-time PCR, flow cytometry, confocal microscopy (CM), as well as [^{35}S]-sulfate metabolic labeling of sulfated GAGs (Fig. S1A–D). The Syn4 knockdown did not affect the expression of von Willebrand factor, a typical EC marker (Fig. S1E). Furthermore, the mRNA levels of Syn4 were re-established when cells were grown for 7 and 14 days without antibiotic pressure (Fig. S2A). Also, protein expression and cellular localization of Syn1, 2 and 3 were evaluated by flow cytometry and confocal microscopy. The expression of other members of the Syndecans family was also investigated. The low mRNA levels for the other family members (Fig. S3A–C), does not implicate in low levels of the proteins. Both flow cytometry (Fig. S3D, F, H) and confocal microscopy (Fig. S3E, G, I) showed no alterations in the protein levels of the Syndecan-1, Syndecan-2 and Syndecan-3 after Syndecan-4 knockdown.

Owing to the fact that Syndecans are crucial for proper cytoskeleton organization [4,8,14,18], actin fibers were labeled and examined by CM and further structural analysis was performed using ImageJ software [3]. This approach measures and quantifies branches in different pixel/voxel categories, comprising the actin filament organization. Analysis of the tagged skeleton image that represent a binary image from the ROI of the actin network (Fig. 1A), indicated that wild type EC cells display more junctions (green) and slab voxels (blue), 2.5 and 1.3-more respectively, compared to shRNA-Syn4-EC cells (Fig. 1A and B). The number and length of branches confirmed these results (Fig. 1B). The number of junction voxels and slab voxels inside of EC cells results in a superior number of branches when compared to Syn4 knockdown cells, indicating that EC cells form structured actin bundle networks. In shRNA-Syn4-EC cells, most junction voxels are present in filopodial protrusions resulting in a tight cell-cell adhesion (Fig. 1A, tagged skeleton image). shRNA-Syn4-EC cells displayed significantly longer branches (2.5-fold) than EC cells (Fig. 1B), confirming, once again, that EC cells present more branches within the cells, unlike shRNA-Syn4-EC cells, that show structured and long filopodial protrusions.

Further analyses were conducted using super-resolution microscopy. This technique exploits the 20 nm lateral resolution of the GSD system, enabling measurement of the width of the actin filaments. Indeed, the difference between the two cells is prominent (Fig. 1C). EC cells displayed thicker actin filaments in cells (50 to 140 nm) (Fig. S4A) and fewer filopodial protrusions, while in contrast, shRNA-Syn4-EC cells, showed longer filopodia, 200–250 nm thick (Fig. S4B).

Syndecan-4 loss affects the focal adhesion and decouples vinculin from the actin filaments

Syn4 as well as integrins are known to be essential for FA formation [7,12,15,16,19,25,48]. As expected and in agreement with studies undertaken in different cell lines, the knockdown of Syn4 resulted in loss of focal adhesion kinase (FAK) in the cellular leading edges compared to EC, where FAK is localized at FA complexes (Fig. 2, arrows and three-dimensional, 3D). Real-time PCR and flow cytometry analysis also confirmed the low expression of FAK for shRNA-Syn4-EC cells (Fig. S5A and B). To further investigate the FA formation, two F-actin associated proteins, vinculin and paxillin were studied. EC cells showed vinculin coupled to F-actin throughout the cell (Fig. 3A, arrows), while shRNA-Syn4-EC cells displayed vinculin predominantly coupled to F-actin at the cell leading edges (Fig. 3 A, arrows). Furthermore, the normal pattern disposition of vinculin was restored when shRNA-Syn4-EC cells were cultured without selective antibiotic pressure (Fig. S2B). Super-resolution microscopy revealed how and where vinculin is associated to F-actin in both cells. EC cells showed vinculin coupled to F-actin filaments (Fig. 3B and Video S1), as suggested by CM, whereas

Please cite this article as: R.P. Cavalheiro, et al., Coupling of vinculin to F-actin demands Syndecan-4 proteoglycan, Matrix Biol (2016), http://dx.doi.org/10.1016/j.matbio.2016.12.006

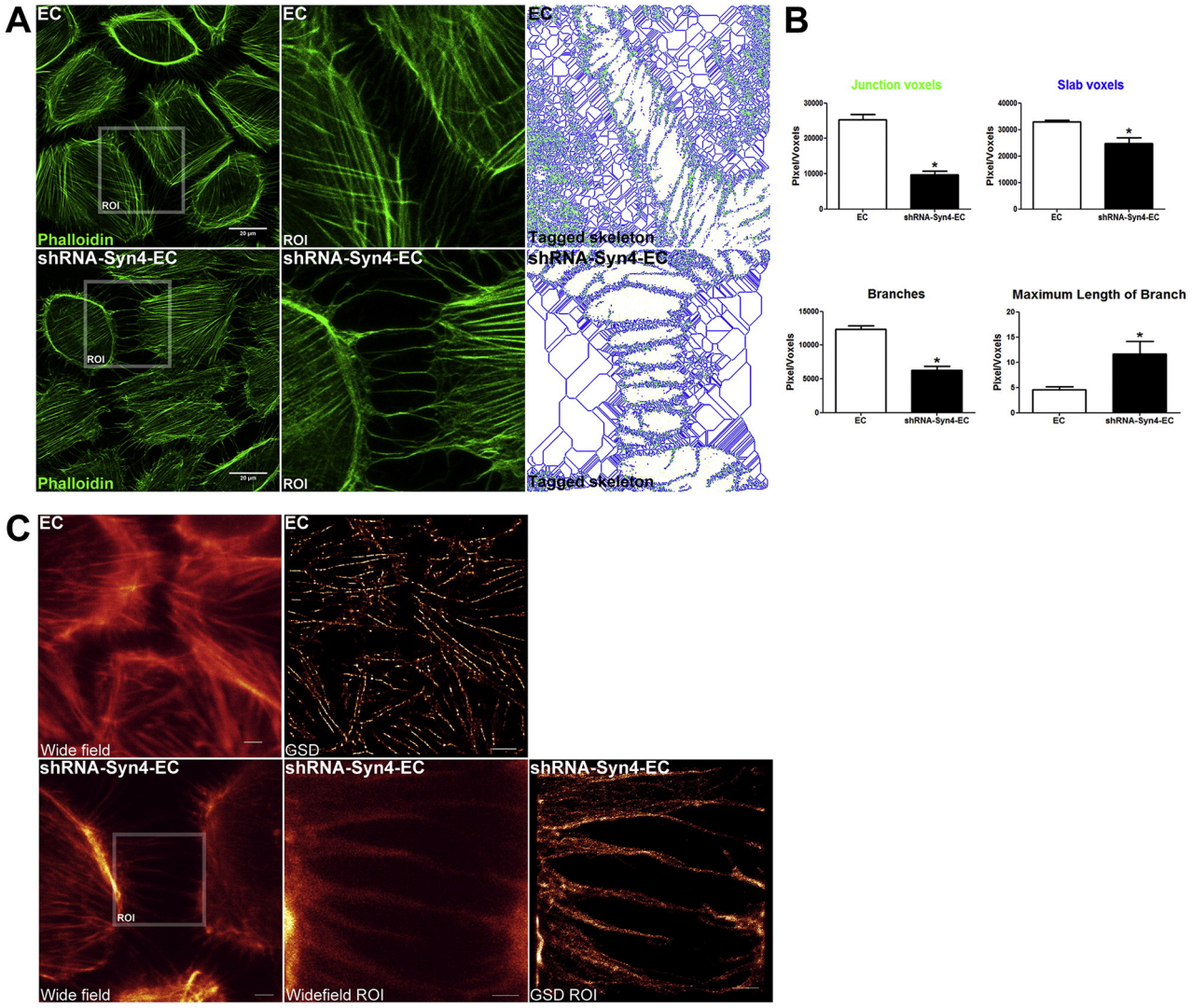

Fig. 1. Syndecan-4 loss in endothelial cells alters actin network causing filopodial protrusions. (A–B) EC and shRNA-Syn4-EC were labeled with Phalloidin Alexa Fluor® 488 and actin network visualized after CM analysis. ROI CM images from both cells were submitted to skeleton analysis using a specific plugin displayed in ImageJ software. EC exhibit more structured actin network at the protrusive lamellipodia when compared to shRNA-Syn4-EC, as shown by the higher number of junction voxels (green) and slab voxels (blue). Wild type cells present higher number of branches at the lamellipodia of the cells, while shRNA-Syn4-EC cells present higher maximum length of branch in the lamellipodia and higher number of branches in the filopodia. Bar: 20 μm. $^{*}p < 0.05$ (paired *t*-test). (C) EC and shRNA-Syn4-EC were cultured on 1.5 high precision round coverslips, fixed with glutaraldehyde, permeabilized and actin network stained using Phalloidin Alexa® Fluor 488 or 647. The super-resolution Ground State Depletion (GSD) images confirm that EC present the actin network within the cells, whereas shRNA-Syn4-EC show structured filopodial protrusions. Bars in wide field images: 5 μm; Bars in ROI images: 2 μm. ROI: region of interest. (For interpretation of the references to colour in this figure legend, the reader is referred to the web version of this article.)

shRNA-Syn4-EC presented vinculin scattered throughout the cytoplasm and associated with F-actin only at the cell leading edges (Fig. 3B and Video S2). On the other hand, no changes in paxillin distribution were observed for both cells (Fig. S6). Thus, Syn4 knockdown affects only vinculin distribution regarding F-actin associated proteins.

Syndecan-4 knockdown affects the distribution and expression of β1 integrin and fibronectin

β1 integrin, a typical transmembrane protein responsible for the integration between ECM and cells, was also investigated, being predominantly localized in a perinuclear region of shRNA-Syn4-EC cells (Fig. 4A,

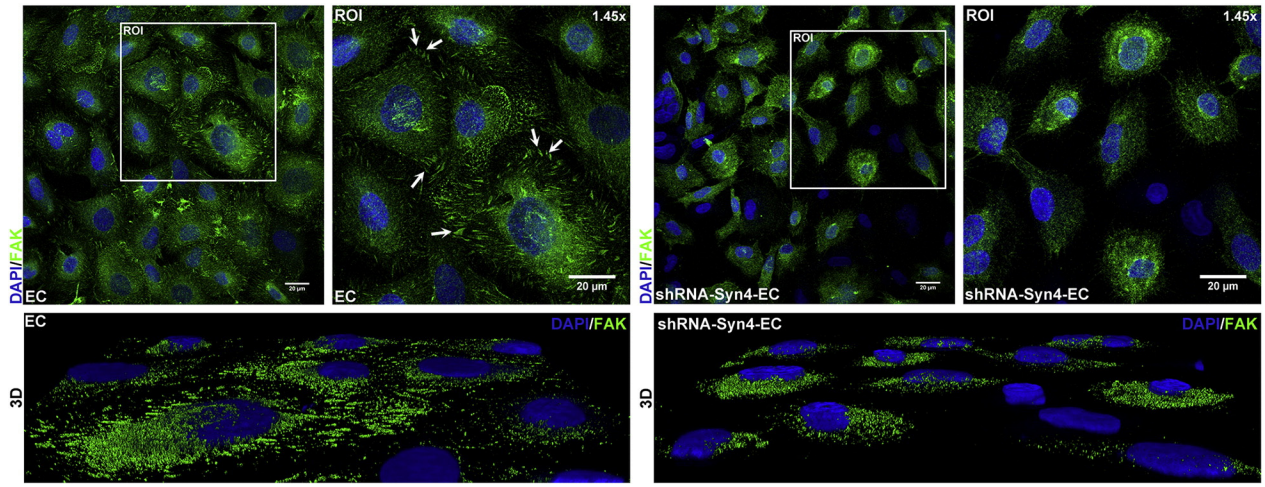

Fig. 2. The knockdown of Syndecan-4 led to loss of FA complexes at the cellular leading edges. EC and shRNA-Syn4-EC were cultured on glass coverslips, immunostained with the anti-FAK (green) and analyzed by CM. Nuclei were stained with DAPI (blue). FAK is located in structures known as FA (arrows). The ROI in the upper panels corresponds to 1.45× zoom and in the lower panel to the 3D projection from the Z stack of the same ROI, which enhanced image details. Bar: 20 μm. ROI: region of interest. (For interpretation of the references to colour in this figure legend, the reader is referred to the web version of this article.)

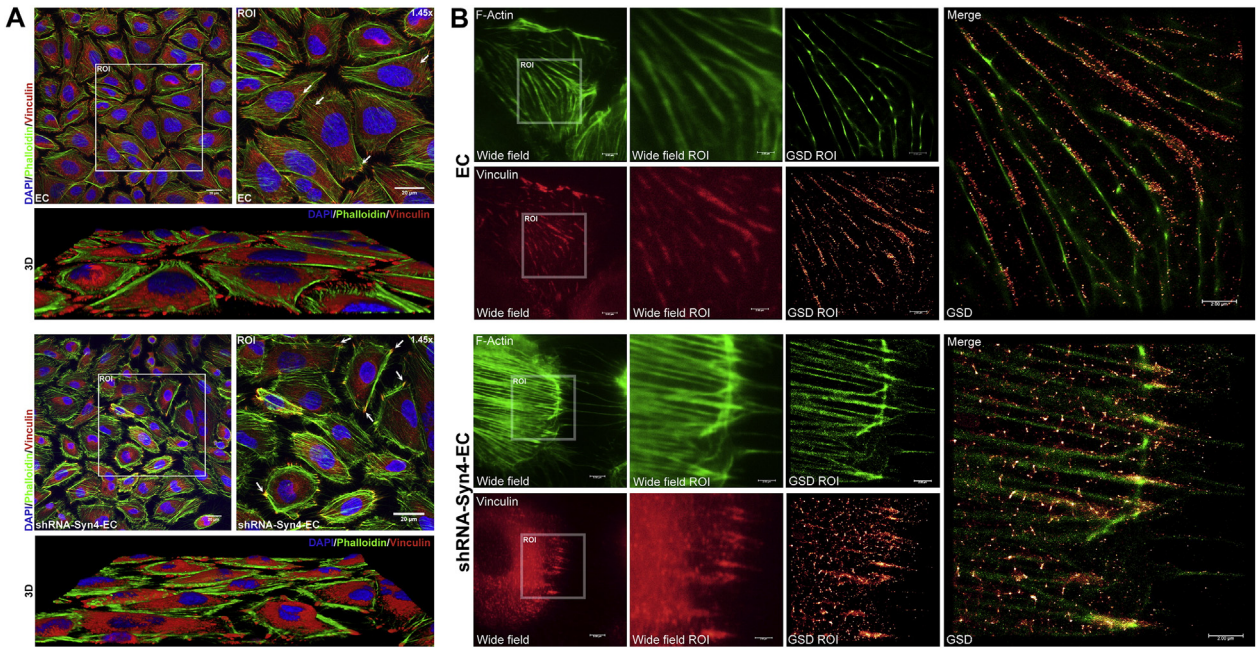

Fig. 3. Syndecan-4 knockdown led to vinculin decoupling from F-actin filaments in endothelial cells. (A) Both cells were cultured on glass coverslips, incubated with anti-vinculin antibody and revealed by secondary antibody conjugated with Alexa Fluor® 647 (red). F-actin filaments were stained with Alexa Fluor® 488 Phalloidin (green) and the nuclei with DAPI (blue). The CM image shows that vinculin is predominantly coupled to F-actin at the leading cell edges for shRNA-Syn4-EC (arrows), while EC cells possess vinculin coupled to F-actin throughout the cell (arrows). The ROI images correspond to 1.45× zoom and in the lower panel to the 3D projection from Z stack of the same ROI, which enhanced image details. Bar: 20 μm. (B) Both cells were cultured on 1.5 high precision round coverslips, incubated with anti-vinculin primary antibody and revealed by Alexa® Fluor 532 or 647. Actin was stained using Phalloidin Alexa® Fluor 488, and afterwards analyzed by wide field and GSD. Bars in wide field images: 5 μm; Bars in ROI images: 2 μm. ROI: region of interest. (For interpretation of the references to colour in this figure legend, the reader is referred to the web version of this article.)

Please cite this article as: R.P. Cavalheiro, et al., Coupling of vinculin to F-actin demands Syndecan-4 proteoglycan, Matrix Biol (2016), http://dx.doi.org/10.1016/j.matbio.2016.12.006

arrows and 3D), contrasting to the wild type cells, in which β1 integrin distribution occurs over the entire cell surface (Fig. 4A and 3D). Real-time PCR showed β1 integrin decreased mRNA in shRNA-Syn4-EC cells when compared to wild type cells (Fig. S5C); however, no differences were observed in total protein expression (Fig. S5D).

Vinculin has been implicated in correct fibronectin deposition at the ECM compartment [43]. Using CM, it was shown that shRNA-Syn4-EC cells displayed low levels of FN fibril structures in the ECM (Fig. 4B and 3D, arrows); accompanied by low mRNA levels and fibronectin expression by SDS-PAGE/immunoblotting (Fig. S5E and F). Again, the expression of fibronectin was reversed when cells were cultured without antibiotic pressure (Fig. S2C). The loss of Syn4 and subsequent alterations in vinculin-actin complex, β1 integrin distribution and FN deposition in the ECM affects cell–matrix communication drastically, reflected in cytoskeletal disorganization and, consequently, cell morphology, all of which were reversed when cells were cultured without antibiotic selection (Fig. S2A–D).

Syndecan-4 knockdown alters the endothelial cell physiology

Cell adhesion

Since shRNA-Syn4-EC cells do not properly deposit FN, show misplaced FA complexes and present altered

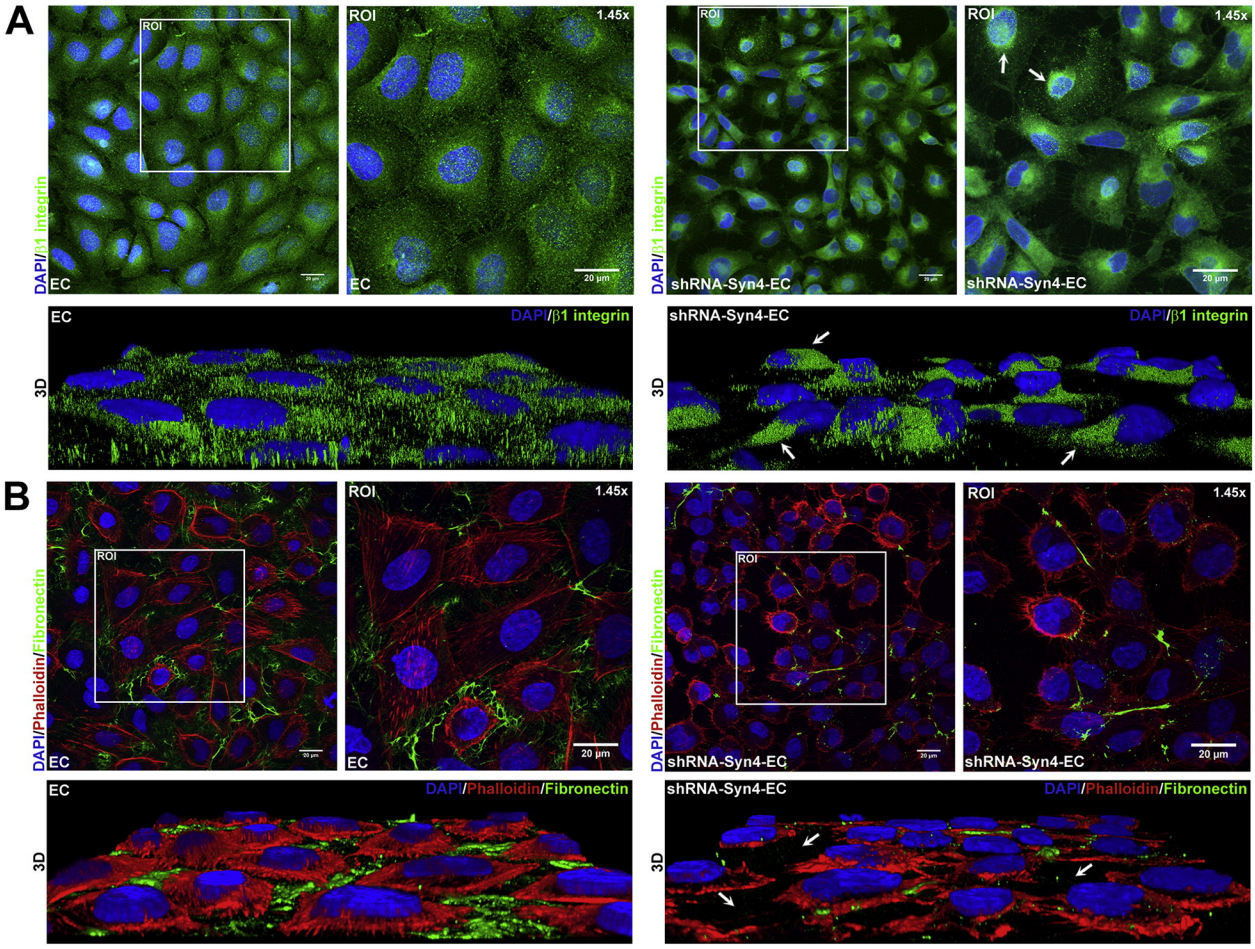

Fig. 4. Syndecan-4 knockdown alters cellular localization of β1 integrin and decreases fibronectin deposition in the ECM. (A) EC and shRNA-Syn4-EC were cultured on glass coverslips, fixed with 2% paraformaldehyde and the cells were permeabilized prior to incubation with the anti-β1 integrin antibody and Alexa® Fluor 488 (green). Nuclei were stained with DAPI (blue). β1 integrin distribution is predominantly localized in a perinuclear region for shRNA-Syn4-EC cells (arrows). The ROI images correspond to 1.45× zoom and in the lower panel to the 3D projection from the Z stack of the same ROI, which enhanced image details. (B) The cells were immunostained with anti-FN (green) and phalloidin (red). Nuclei were stained with DAPI (blue). Syn4 loss decreased the expression of FN in the ECM (3D projection, arrows) and altered actin filaments arrangement. The ROI images correspond to 1.45× zoom and in the lower panel to the 3D projection from the Z stack of the same ROI, which enhanced image details. Bar: 20 μm. ROI: region of interest. (For interpretation of the references to colour in this figure legend, the reader is referred to the web version of this article.)

Please cite this article as: R.P. Cavalheiro, et al., Coupling of vinculin to F-actin demands Syndecan-4 proteoglycan, Matrix Biol (2016), http://dx.doi.org/10.1016/j.matbio.2016.12.006

β1 integrin localization, the ability of the cells to adhere to FN or laminin was assessed. EC cells present dose-dependent adhesion to both substrates while shRNA-Syn4-EC cells showed a striking loss of adhesion to both substrates (Fig. 5A). The distribution of VE-cadherin, an endothelial adhesion molecule that mediates cell-cell adhesion junction formation, was assessed in both cells (Fig. 5B). The shRNA-Syn4-EC, as a consequence of the low FN deposition in the ECM, displayed increased cell-cell VE-cadherin homotypic

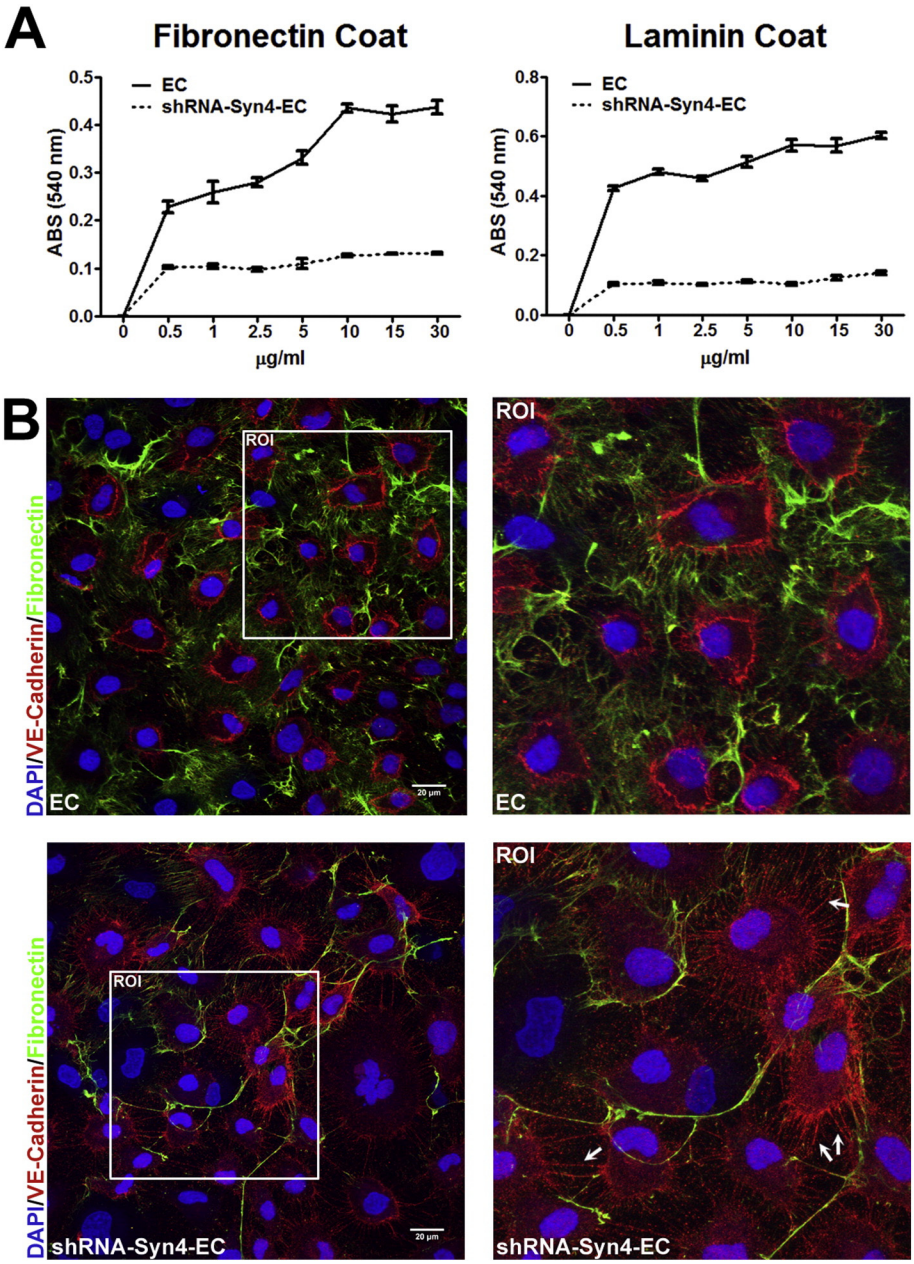

Fig. 5. shRNA-Syn4-EC adhesion to ECM proteins and cell-cell contact via VE-cadherin. (A) EC and shRNA-Syn4-EC were seeded on FN and laminin coats (0–30 µg/ml). Syn4 knockdown led to reduction in the ability of the cells to bind to both ECM glycoproteins. $p < 0.05$ (paired *t*-test). (B) The cells were incubated with anti-VE-cadherin primary antibody revealed by secondary antibody conjugated with Alexa Fluor® 594 (red), and FN primary antibody which was revealed using a secondary antibody conjugated with Alexa Fluor® 488 (green). Nuclei were stained with DAPI (blue). Again, the decrease of FN in the ECM of shRNA-Syn4-EC can be observed. The distribution of VE-cadherin for the Syn4 knockdown cells is mainly at the filopodial protrusions (arrows). Bar: 20 µm. (For interpretation of the references to colour in this figure legend, the reader is referred to the web version of this article.)

Please cite this article as: R.P. Cavalheiro, et al., Coupling of vinculin to F-actin demands Syndecan-4 proteoglycan, Matrix Biol (2016), http://dx.doi.org/10.1016/j.matbio.2016.12.006

interactions, contrasting with the wild type cells (Fig. 5B, arrows). The combined data imply that the loss of Syn4, the low expression as well as the disorganization of FN and actin-associated molecules, leads to increased cell-cell contact.

Cell migration

Chemotaxis assays showed that shRNA-Syn4-EC cells showed increased migration (1.6-fold) towards the chemoattractant (Fig. S7). Hence, the data suggest that Syn4 plays an important role in the cellular adhesion process and its silencing increases the robustness of the migration of ECs.

Capillary-like tube formation

Despite the robust cell migration, shRNA-Syn4-EC cells did not form tube-like structures in matrigel (Fig. S8A). Furthermore, VEGF levels are increased both in the culture media and cell extract (Fig. S8B and C). Together, these data suggest that ordered cell migration is compromised. The decreased capacity of tube formation in Syn4 silenced cells could be related to its lower adhesion ability.

Cell proliferation

Both EC and shRNA-Syn4-EC cells were cultured for 48 h under starvation conditions. Afterwards, the cells were supplemented or not with 10% FCS and after 20 h the nuclei counted. The results clearly show that shRNA-Syn4-EC cells exhibit significant higher cell proliferation regardless of the presence of growth factors (Fig. 6). The knockdown of Syndecan-4 in endothelial cells drives the cells to a more robust proliferative status.

Alteration of endothelial cell behavior

The shRNA-Syn4-EC and wild type cells were subjected to anchorage-independent growth. shRNA-Syn4-EC formed three times more colonies in a semisolid environment than wild type EC cells (Fig. S9). Since anchorage independence of growth can correlate with the capacity of cells to form tumors, the effect of the Syn4 silencing in tumor growth was tested by the subcutaneous inoculation of both cells into Balb/c-SCID mice. Wild type EC cells did not induce tumor formation. On the other hand, shRNA-Syn4-EC cells were able to promote tumor formation. Tumor volume measurements were performed every 5 days up to day 30 and tumor volume became stable after 25 days (Fig. S10A). After 30 days, the mice were killed, tumors removed, sectioned and stained with Hematoxylin and Eosin for histochemical analysis, which revealed the presence of vessel-like structures both in transverse and longitudinal planes (Fig. 10SB). The images also showed that these vessels comprised a single layer of EC cells (Fig. 10SB, arrows). Furthermore, the presence of erythrocytes in the lumen of the vessels was also detected (Fig. 10SB, asterisks), indicating that the structures were indeed blood vessels. Finally, tumor sections were also evaluated using CARS microscopy (Fig. 10SC). Lipids in the CARS images are shown in red, representing CH2 asymmetrical bond stretching (2885 cm^{-1}). Second harmonic generation was also used to image collagenous fibers (green). Lipids are mainly present along tumor borders and outline small vessels within the tumor. On the other hand, collagen fibers are restricted to the tumor core. The figure also depicts two different regions from the total scan, where it can be seen small vessels (red) surrounded by collagen fibers with an average length of around 77.5 μm to 95.2 μm (region A), and ample lipid distribution at the tumor borders (region B).

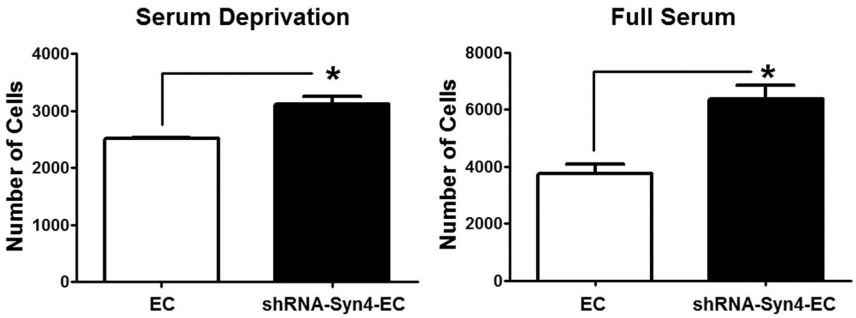

Fig. 6. EC and shRNA-Syn4-EC proliferation assay. Cells (EC and sh-RNA-Syn4-EC) were cultured in 0.2% of FCS for 48 h and total number of cells analyzed (serum deprivation). In the full serum group, cells were also starved for 48 h and subsequently exposed to 10% FCS, maintained for additional 20 h, and total number of cells analyzed (full serum). In both conditions the cells were fixed and incubated with Hoechst (nuclei staining). Total number of cells was obtained using In Cell analyzer 2200 Imaging System (GE Healthcare Life Sciences). The total number of cells was obtained from 9 randomized fields per well (3 wells per group). n = 2–4/group $^*p < 0.05$.

Please cite this article as: R.P. Cavalheiro, et al., Coupling of vinculin to F-actin demands Syndecan-4 proteoglycan, Matrix Biol (2016), http://dx.doi.org/10.1016/j.matbio.2016.12.006

Discussion

Syn4 proteoglycans act as co-receptors, modulating the binding and thus activity of a large number of growth factors and cytokines to their receptors, as well as acting as a bridge between ECM proteins and intracellular signaling molecules [7,12,14,28,29,31,41,42,45,46,50]. The importance of Syn4 to biology is indicated by its ubiquitous distribution in nearly all multicellular organisms and its highly conversed protein sequence, particularly the cytoplasmic domain [14].

In the current study, Syn4 knockdown yielded the successful and specific silencing of the core protein and, consequently, of HS chains. Our findings showed that Syn4 silencing alters endothelial cell biology processes, particularly those associated with actin network arrangement, agreeing with previous data demonstrating that Syn4 null fibroblasts, for instance, have altered actin cytoskeleton with no organization of alpha-smooth muscle actin into bundles [18].

Owing to the facts that Syn4 knockdown altered actin organization and its cytoplasmic domain is well known to interact with cytoskeleton-associated molecules, we further investigated the arrangement of specific cytoskeleton-associated proteins, such as paxillin and vinculin. No significant alterations were observed for paxillin, whereas, vinculin was predominantly coupled to F-actin at the cell leading edges for Syn4 knockdown cells, contrasting with wild type EC where vinculin is coupled to F-actin throughout the cell. Using super-resolution microscopy, in which the relative positions of proteins in cellular structures can be determined [21,22,36,38], it was confirmed that vinculin is actually decoupled from F-actin filaments and scattered throughout the cytoplasm of Syn4 knockdown cells, while wild type cells displayed vinculin coupled to F-actin filaments, at force-bearing FA sites, showing that such effect is geographically and protein selective.

Syn4 silencing affected three main proteins associated with cell motility: FN, β1 integrin and FAK. These cells showed reduced levels of FN in the extracellular environment, altered β1 integrin cellular localization and loss of FA complexes. Furthermore, vinculin has been shown to be required for proper FN deposition throughout the ECM [43], a fact that is reinforced by our results in which FN fibrils are not found in the ECM space of Syn4 depleted cells. Consequently, their cell adhesion ability towards both FN and laminin coats showed that Syn4 is essential for the adhesion of EC to both substrates.

Lamellipodia and filopodia cell protrusions, which are membrane projections supported by the actin machinery that pushes the plasma membrane forward [17,20,24] and are commonly related to cell motility and migration [1,8], were drastically altered by Syn4 knockdown. Cells exhibited significantly structured and extended filopodial protrusions, and concomitant decreases in the actin network. Furthermore, once they had lost the ability to attach to the ECM, the cells focused on new ways of maintaining communication, and ultimately cell survival, evidenced by the distribution of VE-cadherin in Syn4 knockdown in filopodia-like structures in accordance with previous data [2,10]. Additionally, the cell migration results demonstrated that the loose interaction with ECM substrates resulted in robust migration, possibly as a means of cellular survival. Nonetheless, due to the low adhesion of the Syn4 knockdown cells the increased migration did not imply in proper cell orientation to form tube-like structures.

Several studies have described the role of Syndecans in tumor cell lines, showing that their knockdown can suppress or enhance tumor growth, invasion and progression [5,11,26,32,34,35,37,39,49]. Accordingly, we showed that Syn4 knockdown supported robust EC growth and colony formation in a semisolid environment, and induced tumor formation in mice that were studied by hematoxylin and eosin staining and coherent anti-stokes Raman scattering microscopy techniques, revealing that the cell masses were highly vascularized; nonetheless, it is important to emphasize that no metastatic sites were found.

Together, the data show that the knockdown of Syn-4 leads to several alterations in the FA complex where the decoupling of vinculin from F-actin filaments is demonstrated for the first time. Furthermore, decreased expression and distribution of FN and FAK, together with arrangement of F-actin and β1 integrin clusters were also shown. Ultimately, our data proposes a model in which Syndecan-4 acts as a central mediator which serves as a cell signaling center where ECM (fibronectin), cell surface (integrins) and intracellular components (actin and vinculin) come together, and once Syn4 is silenced, cell adhesion, migration and proliferation are altered, thereby drastically altering normal endothelial cell behavior. The proposed mechanism can be depicted in Fig. 7. Syndecan-4 integrity is essential for normal endothelial cell behavior, being crucial for the interaction of the cells with ECM proteins, such as FN, and the actin cytoskeleton via its cytoplasmic tail. Syndecan-4 in wild type endothelial cells interacts with fibronectin leading to integrin dimerization, which in turn activates FAK a key component of the signal transduction pathways and proper arrangement of the F-actin and associated cytoskeletal proteins, such as paxillin and vinculin in FA. Silencing of Syn4 led to decrease deposition of FN in the endothelial cells ECM and normal β1 integrin disposition at the cell surface and FAK arrangement in the inner plasma membrane, impairing the normal FA complex activation, mainly due to the uncoupling of vinculin to F-actin filaments.

Please cite this article as: R.P. Cavalheiro, et al., Coupling of vinculin to F-actin demands Syndecan-4 proteoglycan, Matrix Biol (2016), http://dx.doi.org/10.1016/j.matbio.2016.12.006

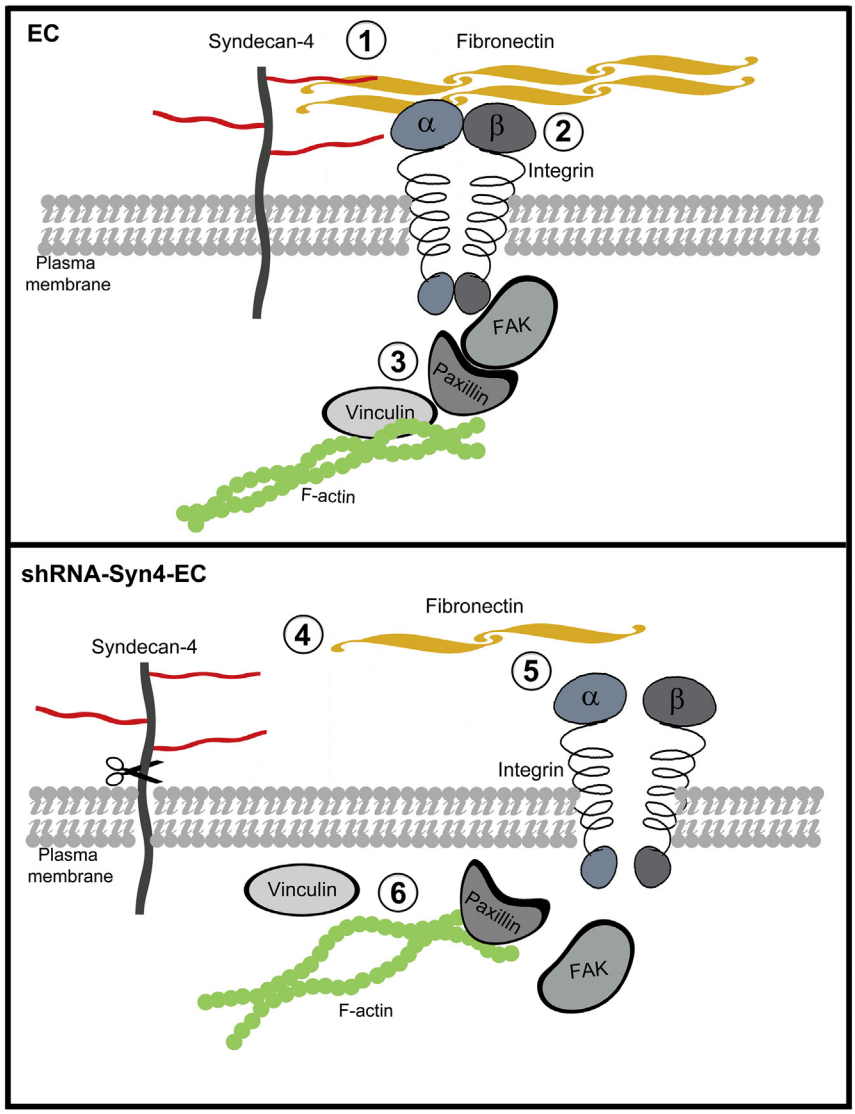

Fig. 7. Syndecan-4 knockdown affects normal focal adhesion complex. Syn4 is essential for normal endothelial cell behavior, being crucial for the interaction of the cells with ECM proteins, such as FN. In the figure, Syn4 in wild type endothelial cells interacts with fibronectin (1) leading to integrin dimerization (2), which in turn activates FAK a key component of the signal transduction pathways and proper arrangement of the F-actin and associated cytoskeletal proteins, such as paxillin and vinculin in FA (3). Silencing of Syn4 led to decrease deposition of FN in the endothelial cells ECM (4) and normal β1 integrin localization at the cell surface (5), FAK arrangement in the inner plasma membrane, impairing the normal FA complex activation, mainly due to the uncoupling of vinculin to F-actin filaments (6).

Methods

Cell line

The wild type endothelial cell (EC) line derived from rabbit aorta [30] was maintained in F12 medium (Gibco BRL) supplemented with 10% FCS (Cultilab), streptomycin and penicillin (both 100 IU/ml) (Sigma–Aldrich) at 37 °C in a humidified atmosphere (2.5% CO_2).

Short hairpin RNA (shRNA) design and transfection

Syn4 specific target sequence (GeneBank Accession No. NM_012649; ^{659}GGGAGAGGAGTTGAG GATT^{677}) was chosen according to online RNAi tools (Integrated DNA Technologies (http://www.idtdna.com)) using the Synthetic double strand oligonucleotides, forward: 5′ACCGGGGAGAG-GAGTTGAGGAT-TTTCAAGAGAAATCCT-CAACTCCTCTCCCTTTTTC3′; reverse: 5′

Please cite this article as: R.P. Cavalheiro, et al., Coupling of vinculin to F-actin demands Syndecan-4 proteoglycan, Matrix Biol (2016), http://dx.doi.org/10.1016/j.matbio.2016.12.006

TGCAGAAA-AAGGGAGAGGAGTTGAG-GATTTCTCTTGAAAATCCTCAACTCCTCTCCC3′. The oligonucleotides were annealed into psiSTRIKE ™ Hygromycin Vector (Promega), cloned into *Escherichia coli* DH5α competent cells and the vectors purified using Gene JET™ Plasmid Miniprep kit (Fermentas). The EC cells (50–80% confluence) were transfected with shRNA-Syn4 vectors using lipofectamine (Invitrogen; manufacturer's specifications). Transfectant cells were selected using 0.1 mg/ml hygromycin B (Roche Applied Science) in F12 medium supplemented with 10% FCS. The empty vector was used as a negative control.

RNA extraction and real-time reverse transcription–PCR analysis

Total RNA was isolated from cultured cells (EC and shRNA-Syn4-EC) using TRIzol® Reagent (Invitrogen), spectrophotometrically quantified and used as the template for the reverse transcriptase reaction. Complementary DNA (cDNA) was reverse transcribed using 2 μg of total RNA and the kit Improm II ™ ReverseTranscriptase (Promega, manufacturer's protocol). Quantitative RT–PCR amplification was performed on 2 μl of diluted cDNA with specific primers for Syndecans 1, 2, 3 and 4, FAK, β1 integrin and fibronectin (Supplementary material Table 1) and the kit Syber Green Master Mix (Applied Biosystems, Foster City, CA) in a 7500 Real-Time PCR System (Applied Biosystems, Warrington, UK), using the activation cycle: 95 °C (10 min), 40 cycles of 95 °C (15 s), 61 °C (1 min), and 72 °C (30 s). Relative expression was analyzed using a standard dilution curve based method for relative real-time PCR data processing performed based on the ΔΔCT method [27]. Results were expressed in arbitrary units and negative controls were used in parallel to confirm the absence of any contamination. Expression values were normalized to the housekeeping gene COX IV (cytochrome *c* oxidase cytochrome *c* oxidase).

Immunofluorescence and confocal microscopy

As described by Trindade et al. [44], EC and shRNA-Syn4-EC (1×10^4) were cultured on glass coverslips (12 mm, 3 days) in 10% FCS prior to use. After washing with phosphate-buffered saline (PBS), cells were fixed with 2% paraformaldehyde (30 min, 22 °C) and washed with 0.1 M glycine. After washing, the cells were incubated with primary antibodies (Supplementary material Table 2) in the presence of 1% BSA (bovine serum albumin) (1 h 30 min, 4 °C). For the detection of Syn1, Syn2, Syn3, Syn4, von Willebrand factor, FAK, VE-cadherin, F-actin, vinculin and paxillin the cells were permeabilized with 0.01% saponin. Secondary antibodies were Alexa Fluor® 488, Alexa Fluor® 594 and Alexa Fluor® 647 (1:250; Molecular Probes). DAPI (4,6-diamidino-2-phenylindole dihydrochloride) was used for nuclear staining (1:10,000; Molecular Probes). F-actin was detected using Alexa Fluor® 488 Phalloidin and Alexa Fluor® 594 Phalloidin (1:200; Molecular Probes). Coverslips were mounted on glass microscope slides using a mounting medium (Fluoromount-G) and images captured with a confocal laser scanning microscope (Leica TCS SP8) equipped with a Plan-Apochromat ×63 objective (numerical aperture 1.4) under oil immersion. The images are represented in maximum intensity projections corresponding to the z-series of confocal stacks.

Skeleton analysis of lamellipodia and filopodial structures

Actin maximum intensity projections (*Z*-series of confocal stacks) from EC and shRNA-Syn4-EC were built by ImageJ software. Region of interest (ROI) images were adjusted to the mean threshold, and converted to binary images. 2D skeleton analysis plugin [3] was used to categorize skeleton structures (lamellipodia and filopodia) based on pixels/voxels where voxels are classified depending on their 8 neighbors; ***junction voxels***: if there are >2 neighbors (in green), and ***slab voxels***: if there are exactly 2 neighbors (in blue).

Super-resolution ground state depletion (SR-GSD) microscopy

EC and shRNA-Syn4-EC (1×10^5) were cultured (10% FCS, 37 °C under 2.5% CO_2 for 3 days) on 1.5 high precision round coverslips (18 mm) (Paul Marienfeld GmbH & Co. KG). Confluent cells were rinsed with PBS and fixed in two steps. Initially, cells were incubated in 0.3% glutaraldehyde diluted in PBS and 0.01% saponin diluted in buffer A (5 mM EGTA, 5 mM $MgCl_2$, 5 mM glucose, 10 mM MES, 150 mM NaCl, for 2 min, at room temperature), then incubated in buffer A containing 0.5% glutaraldehyde for 10 min at room temperature. The cells were then treated with 0.1% $NaBH_4$ in PBS for 7 min at room temperature, washed in PBS and incubated with blocking solution (5% BSA in PBS) for 1 h at room temperature. The cells were then incubated with Alexa Fluor® 647, 488 or 532 phalloidin (1:150) in PBS and incubated overnight at 4 °C. The vinculin primary antibody was diluted in PBS containing 5% BSA (1:150), incubated (4 h), washed in PBS for several times and incubated with Alexa Fluor® 647, 488 or 532 (1 h). The coverslips were mounted in depression slides containing embedding medium (70 mM β-mercapto-ethylamine in PBS pH 7.4) and finally analyzed on a Leica SR GSD 3D microscope. Measurements of actin filaments and filopodial structures employed Leica LAS AF software (Leica Microsystems).

Please cite this article as: R.P. Cavalheiro, et al., Coupling of vinculin to F-actin demands Syndecan-4 proteoglycan, Matrix Biol (2016), http://dx.doi.org/10.1016/j.matbio.2016.12.006

Coherent anti-stokes Raman scattering (CARS) microscopy

Tumor tissues were also analyzed using TCS SP8 CARS Confocal Microscope (Leica). The system consists of an inverted microscope (DMI 6000 CS Trino, Leica) equipped with a picoEmerald tunable light source (APE). The excitation light was focused using a plan apochromatic multi-immersion objective (HC PL APO CS2 20×/0.75). The source was tuned to 816.2 nm to resonantly excite the symmetric stretching vibration of methylene groups at 2850 cm^{-1}. Epi-CARS detector was used to detect CH_2 signals, while Epi-SHG was used to detect second harmonic generation from collagen fibers. Images are represented as maximum intensity projections, corresponding to the *Z*-series of confocal stacks and were collected by tile scan and processed with Leica LAS AF software.

Flow cytometry analysis

EC or shRNA-Syn4-EC post-confluent cells (1×10^6) were detached from the culture plate using citric saline solution (135 mM KCl, 15 mM sodium citrate), cells in suspensions were washed several times (PBS), fixed with 2% paraformaldehyde and permeabilized with 0.01% saponin. The cells were then incubated (2 h) with anti-Syn1, anti-Syn2, anti-Syn3, anti-Syn4, anti-FAK and anti-β1 Integrin antibodies when required and were diluted in PBS with1% BSA. The primary antibodies were detected after incubation with fluorescent-labeled secondary antibody (40 min). Data analyses were performed in a FACSCalibur flow cytometer (Becton Dickinson) using the ModFit LT 2.0 software (Verity Software House, Inc.).

Synthesis of [^{35}S]-sulfated glycosaminoglycans

PGs synthesized by the cells (EC and shRNA-Syn4-EC) were metabolically labeled with carrier free [^{35}S]-sulfate (150 μCi/ml) (National Centre for Nuclear Research Radioisotope Centre - Radioisotope Centre POLATOM) in serum-free F12 medium (18 h, 37 °C) in a humidified atmosphere with 2.5% CO_2. The culture-conditioned medium was collected and the cells washed twice with PBS buffer and then scraped from the dish with 3.5 M urea in 25 mM Tris-HCl pH 7.8. The radioactive GAG free chains were prepared from the cell lysates and from the culture medium by incubation with 4 mg of maxatase (Biocon do Brasil Industrial Ltda) (0.1 mg/ml in 0.05 M Tris-HCl pH 8.0 containing 0.15 M NaCl) for 18 h at 60 °C in the presence of carrier HS, chondroitin sulfate and dermatan sulfate (Seikagaku Co.) (100 μg/ml). The sulfated GAGs were identified and quantified by agarose gel electrophoresis as previously described [30]. Radioactive [^{35}S]-GAGs bands were located by exposure of the gels (after fixation, drying and staining) to Cyclone storage phosphor screen (Packard) for 24 h. For quantification, the radioactive bands were scraped off the agarose gels, and counted in 5 ml of Ultima Gold (PerkinElmer) in a liquid scintillation spectrometer. Cell protein was determined using a BCA protein kit assay (Thermo Scientific).

Cell adhesion assay

As described by Carneiro et al. [6], tissue culture plates (96 wells, Costar Corp.) were coated for 2 h with FN or laminin diluted in PBS in different concentrations (2.5, 5, 10 and 30 μg/ml). Non-adhesive substratum was prepared by coating the wells with 1% BSA for 60 min at 37 °C under 2.5% CO_2 atmosphere. The plates were washed with PBS and blocked with 1% BSA in PBS for 1 h. EC or shRNA-Syn4-EC were washed and suspended at 5×10^4 in 0.5 ml F-12 medium and allowed to attach to the substratum for 1 h at 37 °C under 2.5% CO_2 atmosphere. Unattached cells were removed by washing with PBS. Attached cells were fixed in methanol for 20 min, stained with 0.8% crystal violet (Sigma) dissolved in 20% ethanol and washed five times in PBS. The dye was eluted with 50% ethanol in 0.1 M sodium citrate, pH 4.2 and the optical density measured at 540 nm using the SoftMax Pro Software (Molecular Devices Co.) in VersaMax microplate reader (Molecular Devices Co.). This assay was carried out in quadruplicate.

Transwell migration assay

EC and shRNA-Syn4-EC were seeded (5×10^4 in 400 μl F12/well) in the upper chamber of the pre-hydrated transwell insert (24 well plate). The chemoattractant medium (10% FCS) was placed in the lower chamber and the cells incubated at 37 °C under 2.5% CO_2 atmosphere, for 24 h. Then, the wells were washed with PBS and non-migrating cells on the upper chamber removed using a cotton swab. Migrated cells were fixed with 2% paraformaldehyde and nuclei stained with DAPI. Image acquisitions were performed under an inverted microscope (Axiovert 40 CFL, Carl Zeiss) and analyzed using ImageJ software. DAPI fluorescence was adjusted to the mean threshold and migrated cells counted using particle analysis plugin. The cells were counted in five different fields of each well and the assay carried out in triplicate.

Cell proliferation assay

Sub confluent cells (EC and sh-RNA-Syn4-EC) were maintained in 0.2% of FCS for 48 h (Serum Deprivation), the cells were washed three times with

Please cite this article as: R.P. Cavalheiro, et al., Coupling of vinculin to F-actin demands Syndecan-4 proteoglycan, Matrix Biol (2016), http://dx.doi.org/10.1016/j.matbio.2016.12.006

PBS, fixed with 2% paraformaldehyde and incubated with Hoechst for 30 min (nuclei staining). Total number of cells was counted using *In Cell analyzer 2200 Imaging System* (GE Healthcare Life Sciences). In the full serum group, cells were also starved for 48 h and afterwards exposed to 10% FCS for additional 20 h. After this period, the cells were fixed, the nuclei stained with Hoechst and the number of cells counted by the same method. The total number of cells was obtained from 9 randomized fields per well (3 wells per group). $n = 2–4$/group $^*p < 0.05$.

Capillary-like tube formation on reconstituted basement membrane

Matrigel purified from EHS tumor [23] was thawed at 4 °C, and aliquots of 300 µl (15 mg/ml) applied to 24 well plates, which were maintained at 37 °C in a humidified atmosphere with 2.5% CO_2 for 16 h for gelation. EC and shRNA-Syn4-EC (1×10^5 cells) in 500 µl 10% FCS were then seeded on Matrigel plates. The cultures were maintained at 37 °C in a 2.5% CO_2 humidified atmosphere for 24 h. The assay was performed in triplicate. Tube formation was analyzed on Axiovert 40 CFL inverted light microscope (Carl Zeiss) at 5× and 10× magnification [13]. Three images were randomly taken in different areas and quantified by two different observers. The total length of connected cells forming tubular structures on the Matrigel was measured and determined using image analysis software (AxioVision software, Carl Zeiss). The results are expressed as the number of tubes formed as well as mm tube length/cm^2 area.

VEGF measurement

Sub confluent (80%) EC and shRNA-Syn4-EC in 60 mm plates were kept for 24 h in F12 medium at 37 °C in a humidified atmosphere with 2.5% CO_2. Media culture were collected and VEGF quantified using VEGF Quantikine® ELISA kit (R&D Systems) according to the manufacturer's instructions. The VEGF measurements were performed in Wallac VICTOR^2 1420 Multilabel Counter (Perkin Elmer). This assay was carried out in triplicate.

Western blotting

The protein extraction was performed by two different methods, for VEGF analysis, the protein was extracted from confluent EC and shRNA-Syn4-EC cell plates using cell lysis buffer (Cell Signaling) in the presence of protease inhibitors for 2 h on ice. For fibronectin analysis, the ECM was obtained as described [9]. After clearing by centrifugation, protein concentration was determined using a BCA protein kit assay (Thermo Scientific). An equal volume of sodium dodecyl sulfate (SDS) gel loading buffer was added to samples and boiled for 5 min. Protein extracts (50 µg) were resolved by SDS–PAGE and transferred to PVDF membranes (Millipore). Membranes were blocked with 1% fat-free dried milk in Tris-buffered saline anti-COX IV antibody (Supplementary material Table 1). After washing in TBS–T, the primary antibodies were detected by anti-rabbit horseradish peroxidase (HRP)-conjugated secondary antibody (GE Healthcare). The immunoblots were revealed by chemiluminescence with Super Signal reagent (Thermo Scientific). COX IV protein was used for data normalization. The bands were acquired using a gel documentation system (MF-ChemiBIS) and the intensities quantified using the ImageJ software.

Soft agar colony formation

Soft agar assays were performed in 24-well plates. Firstly, an agarose base layer was prepared by addition of 500 µL of 0.6% HGT agarose (Marine Colloids, Inc., High Gelling Temperature) diluted in F12 medium in each well, which were maintained at room temperature until solidification. Afterwards, EC and shRNA-Syn4-EC (1×10^4) were suspended in 500 µL of 0.3% agarose prepared in F12 medium containing 10% FCS and placed on top of the base layer of each well. The cells were allowed to grow at 37 °C in a 2.5% CO_2 humidified atmosphere for 15 days and total colonies ($\geq$ of 6 cells) counted by three distinct analyzers in an inverted light microscope (Axiovert 40 CFL, Carl Zeiss).

Subcutaneous tumor xenografts and assessment of growth

The ability of both EC and shRNA-Syn4-EC cells to induce tumor was tested using Balb/c-SCID mice. Briefly, the cells were harvested, washed in PBS, and subcutaneously injected (2×10^6 EC or shRNA-Syn4-EC in 200 µl of PBS) at the dorsal region of 8-wk-old male SCID mice. For control group only 200 µl of PBS was injected. The animals were kept in 12 h light/12 h dark room conditions with free access to food and water. The mice were monitored for tumor formation over a period of 4 weeks, and tumor size was measured by macroscopic examination using an electronic digital caliper, every 5 days by two independent observers. Tumor volume was calculated as length × width^2. BALB/c-SCID (severe combined immunodeficient) mice were obtained from the animal breeding unit of the Biomedical Institute of Universidade de São Paulo. All experiments were in accordance with the Brazilian Federal Law for Animal Experiments that takes into consideration the 3Rs and were approved by the Animal Care and Ethics Committee of the University (number 0658/05).

Please cite this article as: R.P. Cavalheiro, et al., Coupling of vinculin to F-actin demands Syndecan-4 proteoglycan, Matrix Biol (2016), http://dx.doi.org/10.1016/j.matbio.2016.12.006

Tumor specimens

At the end of the observation period, the mice were killed and tumors were dissected and fixed in 4% buffered paraformaldehyde at 4 °C for 12 h. Afterwards the tumors were submerged in 30% sucrose for 24 h at 4 °C and embedded in tissue conditioning medium (Tissue Tek, Sakura Finetek Inc.). All animals were macroscopically evaluated for tumor growth. Tumor was only detected at the site of inoculation. Tumors were cut in sections (4 μm), washed in PBS and stained with hematoxylin and eosin (H&E). The sections stained with H&E were photographed under an inverted light microscope (Axiovert 40 CFL, Carl Zeiss) at 40× magnification and the sections without stain were analyzed under a TCS SP8 CARS Confocal Microscope.

Statistics

The data are expressed as the mean ± standard error of the mean (SEM). Statistical analyses were performed using paired Student's *t*-tests for comparison between two groups and analysis of variance (ANOVA) by Bonferroni post-test for multiple comparisons among groups. A probability value of $p < 0.05$ was considered significant. Statistical analysis was performed with the GraphPad Prism version 5 software package (GraphPad Software).

Supplementary data to this article can be found online at http://dx.doi.org/10.1016/j.matbio.2016.12.006.

Funding

This study was supported by grants from CAPES (Coordenação de Aperfeiçoamento de Pessoal de Nível Superior), CNPq (Conselho Nacional de Desenvolvimento Científico e Tecnológico) and FAPESP (Fundação de Amparo a Pesquisa do Estado de São Paulo) (15/08782-3 and 15/03964-6), Brazil.

Competing interests

We have no competing interests.

Authors' contributions

RPC carried out the molecular and cellular lab work, participated in data analysis, carried out sequence alignments, participated in the design of the study and drafted the manuscript; ILST conceived cellular transformation experiments. TRJB, CCL, VJCT, GMV and JLD conducted the cellular experiments. MAL, EAY and HBN conceived, designed and coordinated the study, and helped draft the manuscript. All authors gave their final approval for publication.

Received 15 August 2016;
Received in revised form 4 November 2016;
Accepted 4 December 2016
Available online xxxx

Keywords:
Heparan sulfate;
β1 integrin;
Fibronectin;
Focal adhesion proteins;
Super-resolution microscopy;
Actin network

Abbreviations used:
CARS, coherent anti-stokes Raman Scattering; CM, confocal microscopy; EC, endothelial cells; ECM, extracellular matrix; FA, focal adhesion; FAK, focal adhesion kinase; FCS, fetal calf serum; FN, fibronectin; GAG, glycosaminoglycans; HS, heparan sulfate; HSPG, heparan sulfate proteoglycans; PG, proteoglycans; ROI, region of interest; shRNA, short hairpin RNA; shRNA-Syn4-EC, Syndecan-4 silenced endothelial cells; Syn4, Syndecan-4; 3D, three-dimensional; SDS-PAGE, sodium dodecylsulfate polyacrylamide gel electrophoresis; VEGF, vascular endothelial growth factor.

References

[1] J.C. Adams, Regulation of protrusive and contractile cell-matrix contacts, J. Cell Sci. 115 (2002) 257–265.
[2] S. Almagro, C. Durmort, A. Chervin-Petinot, S. Heyraud, M. Dubois, O. Lambert, C. Maillefaud, E. Hewat, J.P. Schaal, P. Huber, D. Gulino-Debrac, The motor protein myosin-X transports VE-cadherin along filopodia to allow the formation of early endothelial cell-cell contacts, Mol. Cell. Biol. 30 (2010) 1703–1717.
[3] I. Arganda-Carreras, R. Fernandez-Gonzalez, A. Munoz-Barrutia, C. Ortiz-De-Solorzano, 3D reconstruction of histological sections: application to mammary gland tissue, Microsc. Res. Tech. 73 (2010) 1019–1029.
[4] P.C. Baciu, S. Saoncella, S.H. Lee, F. Denhez, D. Leuthardt, P.F. Goetinck, Syndesmos, a protein that interacts with the cytoplasmic domain of syndecan-4, mediates cell spreading and actin cytoskeletal organization, J. Cell Sci. 113 (Pt 2) (2000) 315–324.
[5] D.M. Beauvais, A.C. Rapraeger, Syndecans in tumor cell adhesion and signaling, Reprod. Biol. Endocrinol. 2 (2004) 3.
[6] B.R. Carneiro, P.C. Pernambuco Filho, A.P. Mesquita, D.S. da Silva, M.A. Pinhal, H.B. Nader, C.C. Lopes, Acquisition of anoikis resistance up-regulates syndecan-4 expression in endothelial cells, PLoS One 9 (2014), e116001.
[7] L. Caseli, R.P. Cavalheiro, H.B. Nader, C.C. Lopes, Probing the interaction between heparan sulfate proteoglycan with biologically relevant molecules in mimetic models for cell membranes: a Langmuir film study, Biochim. Biophys. Acta 1818 (2012) 1211–1217.

[8] R. Chakravarti, V. Sapountzi, J.C. Adams, Functional role of syndecan-1 cytoplasmic V region in lamellipodial spreading, actin bundling, and cell migration, Mol. Biol. Cell 16 (2005) 3678–3691.
[9] P. Colburn, E. Kobayashi, V. Buonassisi, Depleted level of heparan sulfate proteoglycan in the extracellular matrix of endothelial cell cultures exposed to endotoxin, J. Cell. Physiol. 159 (1994) 121–130.
[10] M. Corada, M. Mariotti, G. Thurston, K. Smith, R. Kunkel, M. Brockhaus, M.G. Lampugnani, I. Martin-Padura, A. Stoppacciaro, L. Ruco, D.M. McDonald, P.A. Ward, E. Dejana, Vascular endothelial-cadherin is an important determinant of microvascular integrity in vivo, Proc. Natl. Acad. Sci. U. S. A. 96 (1999) 9815–9820.
[11] J.R. Couchman, S. Gopal, H.C. Lim, S. Norgaard, H.A. Multhaupt, Syndecans: from peripheral coreceptors to mainstream regulators of cell behaviour, Int. J. Exp. Pathol. 96 (2015) 1–10.
[12] J.L. Dreyfuss, C.V. Regatieri, T.R. Jarrouge, R.P. Cavalheiro, L.O. Sampaio, H.B. Nader, Heparan sulfate proteoglycans: structure, protein interactions and cell signaling, An. Acad. Bras. Cienc. 81 (2009) 409–429.
[13] J.L. Dreyfuss, C.V. Regatieri, M.A. Lima, E.J. Paredes-Gamero, A.S. Brito, S.F. Chavante, R. Belfort Jr., M.E. Farah, H.B. Nader, A heparin mimetic isolated from a marine shrimp suppresses neovascularization, J. Thromb. Haemost. 8 (2010) 1828–1837.
[14] A. Elfenbein, M. Simons, Syndecan-4 signaling at a glance, J. Cell Sci. 126 (2013) 3799–3804.
[15] J.D. Esko, S.B. Selleck, Order out of chaos: assembly of ligand binding sites in heparan sulfate, Annu. Rev. Biochem. 71 (2002) 435–471.
[16] J.W. Franses, E.R. Edelman, The evolution of endothelial regulatory paradigms in cancer biology and vascular repair, Cancer Res. 71 (2011) 7339–7344.
[17] T.M. Gomez, P.C. Letourneau, Actin dynamics in growth cone motility and navigation, J. Neurochem. 129 (2014) 221–234.
[18] S. Gopal, A. Bober, J.R. Whiteford, H.A. Multhaupt, A. Yoneda, J.R. Couchman, Heparan sulfate chain valency controls syndecan-4 function in cell adhesion, J. Biol. Chem. 285 (2010) 14247–14258.
[19] S.L. Gupton, D. Riquelme, S.K. Hughes-Alford, J. Tadros, S.S. Rudina, R.O. Hynes, D. Lauffenburger, F.B. Gertler, Mena binds alpha5 integrin directly and modulates alpha5-beta1 function, J. Cell Biol. 198 (2012) 657–676.
[20] C.A. Heckman, H.K. Plummer III, Filopodia as sensors, Cell. Signal. 25 (2013) 2298–2311.
[21] E. Hoogendoorn, K.C. Crosby, D. Leyton-Puig, R.M. Breedijk, K. Jalink, T.W. Gadella, M. Postma, The fidelity of stochastic single-molecule super-resolution reconstructions critically depends upon robust background estimation, Sci. Rep. 4 (2014) 3854.
[22] B. Huang, H. Babcock, X. Zhuang, Breaking the diffraction barrier: super-resolution imaging of cells, Cell 143 (2010) 1047–1058.
[23] Kleinman, H.K., 2001. Preparation of Basement Membrane Components from EHS Tumors. Current Protocols in Cell Biology / Editorial Board, Juan S. Bonifacino … et al. (Chapter 10, Unit 10 12).
[24] A.L. Law, A. Vehlow, M. Kotini, L. Dodgson, D. Soong, E. Theveneau, C. Bodo, E. Taylor, C. Navarro, U. Perera, M. Michael, G.A. Dunn, D. Bennett, R. Mayor, M. Krause, Lamellipodin and the Scar/WAVE complex cooperate to promote cell migration in vivo, J. Cell Biol. 203 (2013) 673–689.
[25] R.E. Leube, M. Moch, R. Windoffer, Intermediate filaments and the regulation of focal adhesion, Curr. Opin. Cell Biol. 32 (2015) 13–20.
[26] H.C. Lim, H.A. Multhaupt, J.R. Couchman, Cell surface heparan sulfate proteoglycans control adhesion and invasion of breast carcinoma cells, Mol. Cancer 14 (2015) 15.
[27] K.J. Livak, T.D. Schmittgen, Analysis of relative gene expression data using real-time quantitative PCR and the 2(−Delta Delta C(T)) method, Methods 25 (2001) 402–408.
[28] C.C. Lopes, C.P. Dietrich, H.B. Nader, Specific structural features of syndecans and heparan sulfate chains are needed for cell signaling, Braz. J. Med. Biol. Res. 39 (2006) 157–167.
[29] E. Migliorini, D. Thakar, J. Kuhnle, R. Sadir, D.P. Dyer, Y. Li, C. Sun, B.F. Volkman, T.M. Handel, L. Coche-Guerente, D.G. Fernig, H. Lortat-Jacob, R.P. Richter, Cytokines and growth factors cross-link heparan sulfate, Open Biol. 5 (2015).
[30] H.B. Nader, C.P. Dietrich, V. Buonassisi, P. Colburn, Heparin sequences in the heparan sulfate chains of an endothelial cell proteoglycan, Proc. Natl. Acad. Sci. U. S. A. 84 (1987) 3565–3569.
[31] S.S. Nunes, M.A. Outeiro-Bernstein, L. Juliano, F. Vardiero, H.B. Nader, A. Woods, C. Legrand, V. Morandi, Syndecan-4 contributes to endothelial tubulogenesis through interactions with two motifs inside the pro-angiogenic N-terminal domain of thrombospondin-1, J. Cell. Physiol. 214 (2008) 828–837.
[32] M.P. O'Connell, J.L. Fiori, E.K. Kershner, B.P. Frank, F.E. Indig, D.D. Taub, K.S. Hoek, A.T. Weeraratna, Heparan sulfate proteoglycan modulation of Wnt5A signal transduction in metastatic melanoma cells, J. Biol. Chem. 284 (2009) 28704–28712.
[33] E. Okina, T. Manon-Jensen, J.R. Whiteford, J.R. Couchman, Syndecan proteoglycan contributions to cytoskeletal organization and contractility, Scand. J. Med. Sci. Sports 19 (2009) 479–489.
[34] R. Ramnath, R.R. Foster, Y. Qiu, G. Cope, M.J. Butler, A.H. Salmon, P.W. Mathieson, R.J. Coward, G.I. Welsh, S.C. Satchell, Matrix metalloproteinase 9-mediated shedding of syndecan 4 in response to tumor necrosis factor alpha: a contributor to endothelial cell glycocalyx dysfunction, FASEB J. 28 (2014) 4686–4699.
[35] R.M. Reijmers, R.W. Groen, H. Rozemuller, A. Kuil, A. de Haan-Kramer, T. Csikos, A.C. Martens, M. Spaargaren, S.T. Pals, Targeting EXT1 reveals a crucial role for heparan sulfate in the growth of multiple myeloma, Blood 115 (2010) 601–604.
[36] M.J. Rust, M. Bates, X. Zhuang, Sub-diffraction-limit imaging by stochastic optical reconstruction microscopy (STORM), Nat. Methods 3 (2006) 793–795.
[37] K. Shimada, M. Nakamura, M.A. De Velasco, M. Tanaka, Y. Ouji, N. Konishi, Syndecan-1, a new target molecule involved in progression of androgen-independent prostate cancer, Cancer Sci. 100 (2009) 1248–1254.
[38] H. Shroff, C.G. Galbraith, J.A. Galbraith, H. White, J. Gillette, S. Olenych, M.W. Davidson, E. Betzig, Dual-color superresolution imaging of genetically expressed probes within individual adhesion complexes, Proc. Natl. Acad. Sci. U. S. A. 104 (2007) 20308–20313.
[39] M.A. Soares, F.C. Teixeira, M. Fontes, A.L. Areas, M.G. Leal, M.S. Pavao, M.P. Stelling, Heparan sulfate proteoglycans may promote or inhibit cancer progression by interacting with integrins and affecting cell migration, Biomed. Res. Int. 2015 (2015) 453801.

Please cite this article as: R.P. Cavalheiro, et al., Coupling of vinculin to F-actin demands Syndecan-4 proteoglycan, Matrix Biol (2016), http://dx.doi.org/10.1016/j.matbio.2016.12.006

[40] Y. Song, D.C. McFarland, S.G. Velleman, Syndecan-4 cytoplasmic domain regulation of turkey satellite cell focal adhesions and apoptosis, Mol. Biol. Rep. 39 (2012) 8251–8264.
[41] R. Steinfeld, H. Van Den Berghe, G. David, Stimulation of fibroblast growth factor receptor-1 occupancy and signaling by cell surface-associated syndecans and glypican, J. Cell Biol. 133 (1996) 405–416.
[42] C. Sun, M. Marcello, Y. Li, D. Mason, R. Levy, D.G. Fernig, Selectivity in glycosaminoglycan binding dictates the distribution and diffusion of fibroblast growth factors in the pericellular matrix, Open Biol. 6 (2016).
[43] I. Thievessen, N. Fakhri, J. Steinwachs, V. Kraus, R.S. McIsaac, L. Gao, B.C. Chen, M.A. Baird, M.W. Davidson, E. Betzig, R. Oldenbourg, C.M. Waterman, B. Fabry, Vinculin is required for cell polarization, migration, and extracellular matrix remodeling in 3D collagen, FASEB J. 29 (2015) 4555–4567.
[44] E.S. Trindade, C. Oliver, M.C. Jamur, H.A. Rocha, C.R. Franco, R.I. Boucas, T.R. Jarrouge, M.A. Pinhal, I.L. Tersariol, T.C. Gouvea, C.P. Dietrich, H.B. Nader, The binding of heparin to the extracellular matrix of endothelial cells up-regulates the synthesis of an antithrombotic heparan sulfate proteoglycan, J. Cell. Physiol. 217 (2008) 328–337.
[45] Z. Wang, R.J. Collighan, S.R. Gross, E.H. Danen, G. Orend, D. Telci, M. Griffin, RGD-independent cell adhesion via a tissue transglutaminase-fibronectin matrix promotes fibronectin fibril deposition and requires syndecan-4/2 alpha5-beta1 integrin co-signaling, J. Biol. Chem. 285 (2010) 40212–40229.
[46] S.A. Williams, J.E. Schwarzbauer, A shared mechanism of adhesion modulation for tenascin-C and fibulin-1, Mol. Biol. Cell 20 (2009) 1141–1149.
[47] A. Woods, J.R. Couchman, Syndecan-4 and focal adhesion function, Curr. Opin. Cell Biol. 13 (2001) 578–583.
[48] D. Xu, J.D. Esko, Demystifying heparan sulfate-protein interactions, Annu. Rev. Biochem. 83 (2014) 129–157.
[49] Y. Yang, V. MacLeod, Y. Dai, Y. Khotskaya-Sample, Z. Shriver, G. Venkataraman, R. Sasisekharan, A. Naggi, G. Torri, B. Casu, I. Vlodavsky, L.J. Suva, J. Epstein, S. Yaccoby, J.D. Shaughnessy Jr., B. Barlogie, R.D. Sanderson, The syndecan-1 heparan sulfate proteoglycan is a viable target for myeloma therapy, Blood 110 (2007) 2041–2048.
[50] A. Yayon, M. Klagsbrun, J.D. Esko, P. Leder, D.M. Ornitz, Cell surface, heparin-like molecules are required for binding of basic fibroblast growth factor to its high affinity receptor, Cell 64 (1991) 841–848.
[51] A. Yoneda, J.R. Couchman, Regulation of cytoskeletal organization by syndecan transmembrane proteoglycans, Matrix Biol. 22 (2003) 25–33.

Please cite this article as: R.P. Cavalheiro, et al., Coupling of vinculin to F-actin demands Syndecan-4 proteoglycan, Matrix Biol (2016), http://dx.doi.org/10.1016/j.matbio.2016.12.006